Fabrication of zipping electrostatic actuators incorporating inkjet-printed layers

Grasso, Giulio, Rosset, Samuel, Shea, Herbert

Giulio Grasso, Samuel Rosset, Herbert Shea, "Fabrication of zipping electrostatic actuators incorporating inkjet-printed layers," Proc. SPIE 11587, Electroactive Polymer Actuators and Devices (EAPAD) XXIII, 115871O (22 March 2021); doi: 10.1117/12.2581393

SPIE.

Event: SPIE Smart Structures + Nondestructive Evaluation, 2021, Online Only

Fabrication of zipping electrostatic actuators incorporating inkjet-printed layers

Giulio Grasso[a], Samuel Rosset[b], Herbert Shea[a]
[a]Soft Transducers Laboratory (LMTS), École Polytechnique Fédérale de Lausanne (EPFL), Switzerland;
[b]Biomimetics Laboratory, Auckland Bioengineering Institute, University of Auckland, New Zealand

ABSTRACT

Zipping electrostatic actuators operate by bending flexible electrodes using electrostatic forces. This principle allows the use of a wide range of dielectric and conductive materials. Additive Manufacturing (AM) techniques can be used to fabricate these actuators. The selective direct deposition of multiple materials improves the actuator design flexibility, as customized prototypes can be fabricated without masks and moulds. Here we present the first integration of AM techniques in the fabrication process of Hydraulically Amplified Taxels (HAXELs), a class of electrostatic actuators combining zipping electrodes deformation with the inflation of a stretchable material using fluidic coupling. We use an inkjet printer (jetlab® 4 by MicroFab) to deposit Polydimethylsiloxane (PDMS) as the stretchable material and Ethyl Cellulose as a sacrificial material for fluidic features patterning. We integrate gold-sputtered, laser-cut Mylar foils for the flexible part of the actuator by encapsulating them between the inkjet-printed layers. After dissolving the sacrificial material, a dielectric fluid can be injected in the fabricated actuators. Qualitative evaluation of a fabricated device is reported, showing electrode zipping. The presented fabrication process allows future fabrication of highly integrated actuators having arbitrary shapes.

Keywords: Inkjet printing, Electrostatic actuators, Fluidic actuators

1. INTRODUCTION

Soft actuators exploit the mechanical compliance of stretchable elastomers[1,2]. Of the many soft actuation principles[3,4], electrostatically-driven actuators, such as Dielectric Elastomer Actuators (DEAs)[5,6], Peano-HASELs[7,8], and electro-ribbons[9] stand out terms of efficiency, speed, and silent operation, though they require high electric fields. Zipping actuators[7,9–13] allow for particularly high energy density and offer a larger choice of flexible but generally not stretchable materials.

Hydraulically Amplified Taxel (HAXEL)[14] technology combines zipping electrodes and stretchable materials. A cavity consisting of flexible foil at the edges and of a stretchable membrane at the centre is filled with a dielectric oil. Electrodes are patterned on the foils, leading to zipping when a voltage is applied. As a result, the dielectric liquid is displaced from the periphery to the stretchable central region, creating a bump. Actuators less than 10 mm wide and 1 mm thick and weighing only 90 mg generate 300 mN forces and 500 µm out-of-plane displacements, with specific power of 100 W/kg[14]. Both in-plane and out-of-plane motions are achieved by selective electrode zipping. Array configuration have been demonstrated. HAXELs can be used for haptic feedback systems, complex fluidic arrays and soft robots.

Soft devices are traditionally fabricated by bonding or laminating different layers. Electrodes are deposited in the desired patterns. By adopting Additive Manufacturing (AM) techniques[15,16], a higher degree of design flexibility and complexity is allowed, with architectures not possible by more conventional methods and the possibility to implement design changes directly at software level.

Examples can be found in literature of AM of soft electrostatic machines, with the additive deposition of dielectrics[17–19], electrodes[20,21] or both[22–24]. There is a limited choice in the used materials, which have to satisfy both mechanical and dielectric properties.

We present here the first implementation of Additive Manufacturing techniques in the fabrication process of HAXEL devices. Inkjet printing is used to deposit PDMS for the stretchable layers of the devices, as well as an ethyl cellulose-based

Electroactive Polymer Actuators and Devices (EAPAD) XXIII, edited by Iain A. Anderson, Herbert R. Shea, John D. W. Madden, Proc. of SPIE Vol. 11587, 115871O
 · doi: 10.1117/12.2581393

sacrificial material to define fluidic features. Laser-cut Mylar foils with gold sputtered electrodes are integrated to the printed layers in order to obtain a functioning zipping device.

2. DEVICE DESCRIPTION

In this section, we describe the structure of the fabricated devices, which follow the scheme reported in Figure 1 and 2. Total thickness of the fabricated devices is less than 200 µm, and the thickness of deposited material is 100 µm.

Following the HAXEL principle, the fabricated actuators are fluid-filled pouches made out of flexible insulated electrodes and a stretchable membrane. The bottom electrode is deposited on a PET substrate. A first layer of Polydimethylsiloxane (PDMS) acts as first insulating layer and as base material for subsequent depositions. Sacrificial material is then patterned in order to define the fluidic features required for actuation and filling. This material, based on Ethyl Cellulose, can be dissolved by ethanol, allowing the separation of the adjacent layers. This approach also allows to minimize the distance between zipping layers, as it is limited to the sacrificial material thickness at the channel edges (roughly 3 µm). The top zipping electrodes are deposited on Mylar foils which are placed over a thin, inkjet-printed layer of uncured PDMS acting as glue. The integration of Mylar as flexible support for zipping electrodes allows a more efficient zipping, due to its 2000 times higher stiffness when compared to PDMS (4.2 GPa[25] vs. 2 MPa). Mylar also has dielectric breakdown strength (180 V/µm[25]) which is higher than typical values for PDMS[26]. Both sacrificial material and Mylar foils are then encapsulated with an inkjet-printed PDMS layer, thus providing the stretchable membrane required for actuation. The use of inkjet printing allows the fabrication of electrical vias for connection of the top Mylar electrode to a power supply for actuation.

Each actuator is fabricated along with a planar fluidic inlet for its subsequent filling with the dielectric oil. It consists of a large channel to house a PDMS tube used to bring the fluid to the actuator (either ethanol for dissolving the sacrificial material or the dielectric fluid for actuation). The width is narrowed from 6 mm at the inlet interface to 500 µm at the connection to the actuator pouch, in order to minimize its influence during actuation. To strengthen the channel against tearing, a second PDMS layer is printed over it.

Actuators are fabricated in pairs and are fluidically connected by a 1 mm wide channel. This geometry was chosen for a more controlled channel opening process. Ethanol can be pumped in from one connection and exits from the other one along with dissolved sacrificial material, following a U-shaped circuit. This also enables a faster filling of the actuators with dielectric fluid, as any air bubble can be pushed out.

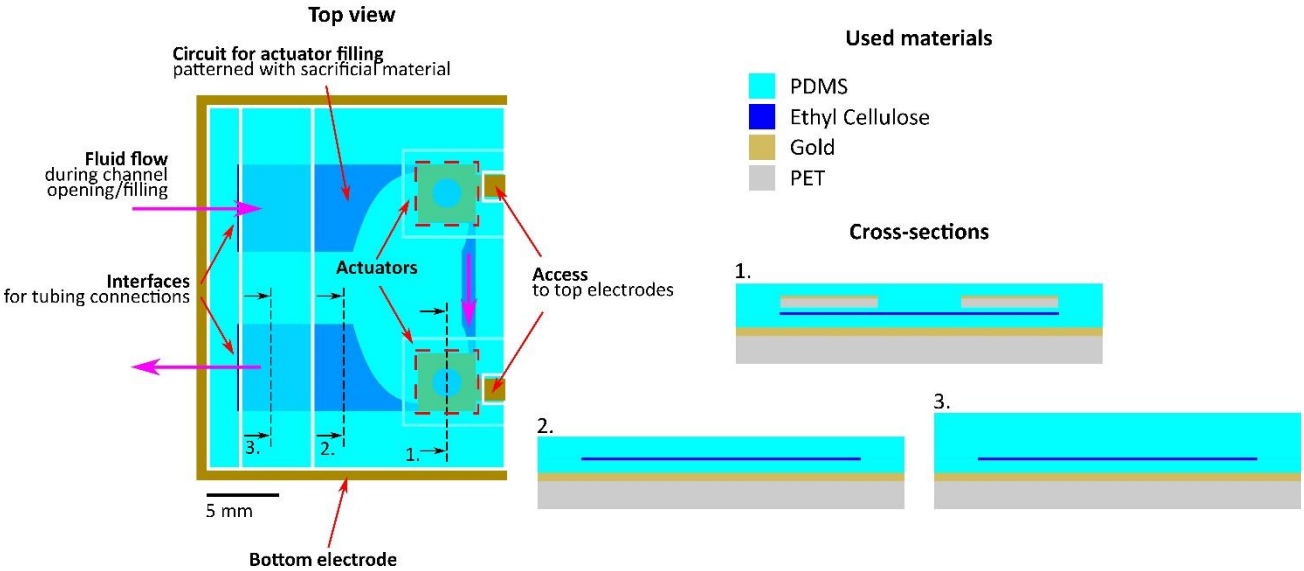

Figure 1. Top view of the zipping actuators, and cross sections at three locations. Fluidic features for actuation and filling are inkjet-printed with Ethyl Cellulose, a sacrificial material that can be dissolved by Ethanol. A U-shaped channel connecting two independent actuators is used for easier channel opening and filling.

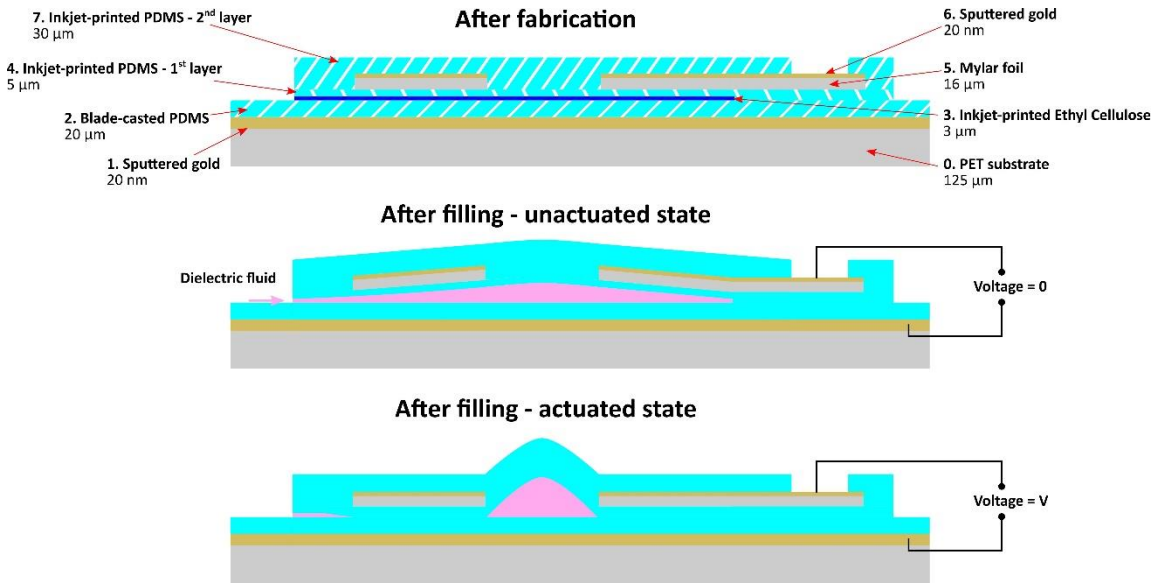

Figure 2. Cross sections of the fabricated actuators showing material and thickness of each layer, before and after dielectric oil filling.

3. FABRICATION PROCESS

Here we now describe the processes adopted for depositing the required materials, as well as the channel opening and filling procedures.

Figure 3 reports the main steps of actuator fabrication. Inkjet printing was performed on a jetlab® 4 from MicroFab. The printable inks and processes are described in a previous publication from our lab[24].

Fabrication occurs in 9 steps:

1. Substrate preparation: a 20 µm thick PDMS (Sylgard® 184 from Dow Corning) is blade casted over a 125 µm PET foil (Melinex ST-506 from Dupont Teijin Films). Test devices were fabricated without a bottom electrode, which is then added by transferring the printed device on a new, gold sputtered PET substrate (see step 9).
2. Sacrificial material patterning: a ink made out of Ethyl Cellulose and Dibutyl Sebacate (Sigma Aldrich) dispersed in ethanol[24] is inkjet printed on the blade-casted PDMS. Blue dye is added to the solvent in order to make the alignment of subsequent layer easier. Actuators are placed close to each other in order to simplify electrical connections.
3. Mylar foil preparation: 15 µm thick PET foil pieces (Mylar® A from Dupont Teijin Films) are sputtered less than 100 nm thick gold. The foils are then laser cut in the desired shape: two sets of zipping electrodes connected together by a strip which will act as contact for the external electrical connection.
4. Bonding layer deposition: an inkjet printable PDMS formulation is obtained by diluting Sylgard® 184 with solvent (Dowsil® OS-2 from Dow Corning) in a 20 wt% solution[24]. Single layers of PDMS are then printed over the actuator squares of the printed sacrificial material, with a 100 µm spacing between droplets and lines. The resulting thickness of these layers is 5 µm.
5. Mylar foil placement: the laser-cut Mylar pieces are aligned with the sacrificial material pattern and placed on the uncured inkjet-printed PDMS with the electrode side facing upwards.
6. Encapsulation deposition: Mylar foils and sacrificial material are encapsulated by an inkjet-printed, 30 µm thick PDMS layer. A 5-pass strategy is adopted in order to achieve a more even surface finish of the layer[24]. Small portions of the sacrificial material are left uncovered in order to allow later tubing insertion. The print job is transferred to an oven and left 2 hours at 80°C for PDMS curing.

7. Stiffeners deposition: the device is placed back on the inkjet printer stage for an additional 30 µm thick PDMS deposition at the tubing interface. This will help preventing tearing of PDMS during insertion of the fluidic connections. The device is then placed in the oven for 2 hours at 80°C.
8. Tubing insertion: a piece of PDMS-based tube (Silastic® Laboratory Tubing 1.2 mm OD from Dow Corning) is cut with a 45 degrees angle from its axis. A small amount of ethanol is placed on the printed channel interfaces, and the trimmed side of the tube is used to gently open the PDMS channel and slid between the PDMS layers. Moisture-curing RTV silicone (Dowsil® 734 from Dow Corning) is applied to seal the channel and to connect the tubing system to the printed device.
9. Transfer onto gold sputtered substrate: the printed stacks are transferred to a new, gold sputtered PET substrate, making sure that the actuators are carefully laminated on it.

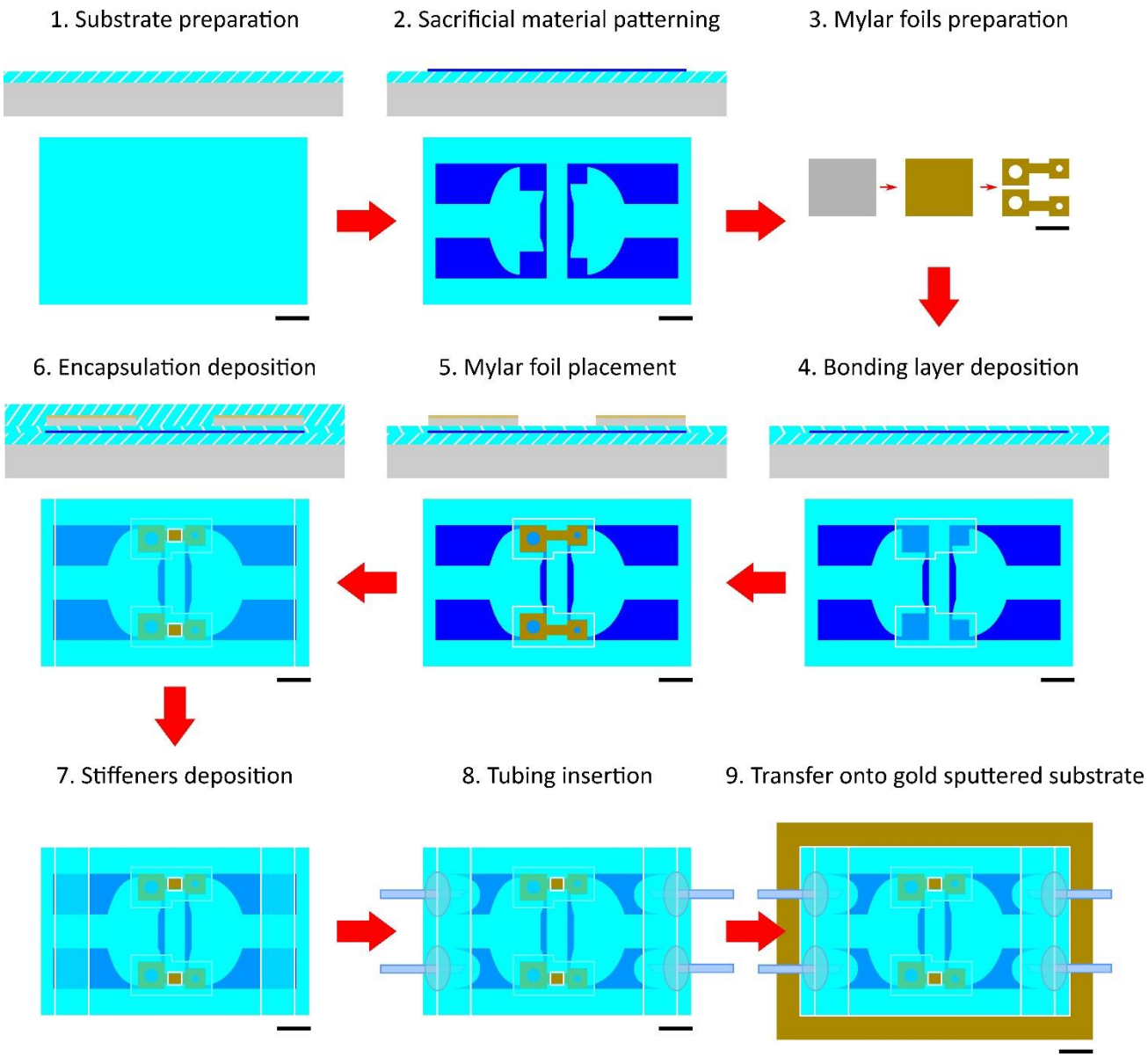

Figure 3. Actuator fabrication (scale bar = 5 mm)

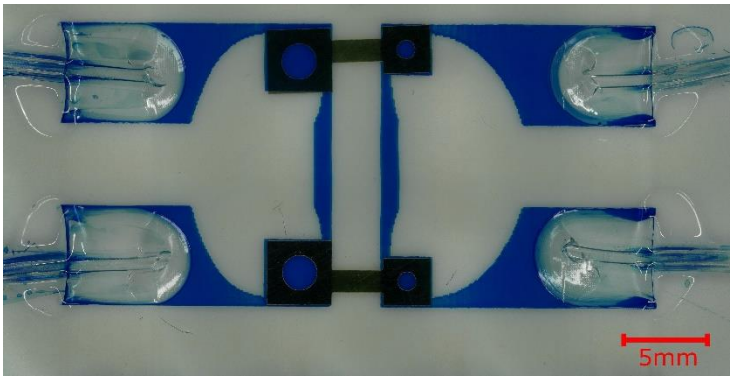

Figure 4. Top view of printed array made out of 4 actuators

The fluidic channels are opened as shown in Figure 5. The device is submerged into an ethanol bath. Ethanol is pressurized to 50 mBar inside the channel using a pneumatic controller (MFCS™-EZ from Fluigent). The ethanol bath is then put in an ultrasonic bath (Sonorex RK 102 H from Bandelin) for 10 minutes to accelerate removal of the sacrificial material, as shown in Figure 6.

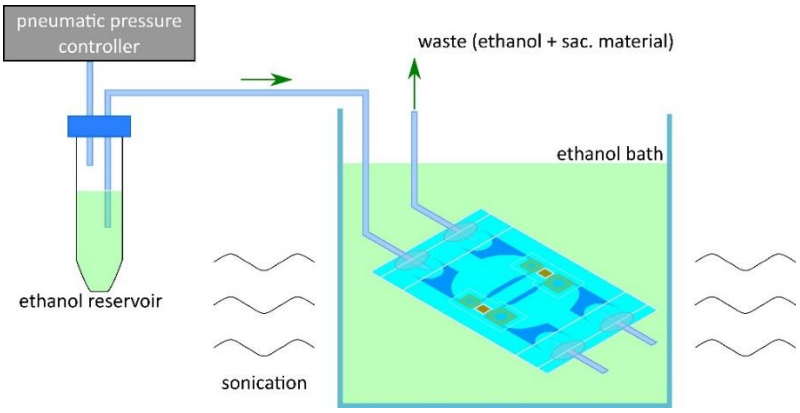

Figure 5. Channel opening process: one device inlet is connected to ethanol reservoir which is then put to a pressure of 50 mBar. The device is submerged into ethanol inside a beaker. The beaker is placed inside an ultrasonic bath, and sonication is performed for 10 minutes. Pressurized ethanol inside the channel will dissolve the sacrificial material even in the narrowest points of the circuit, and will flow out through the second inlet

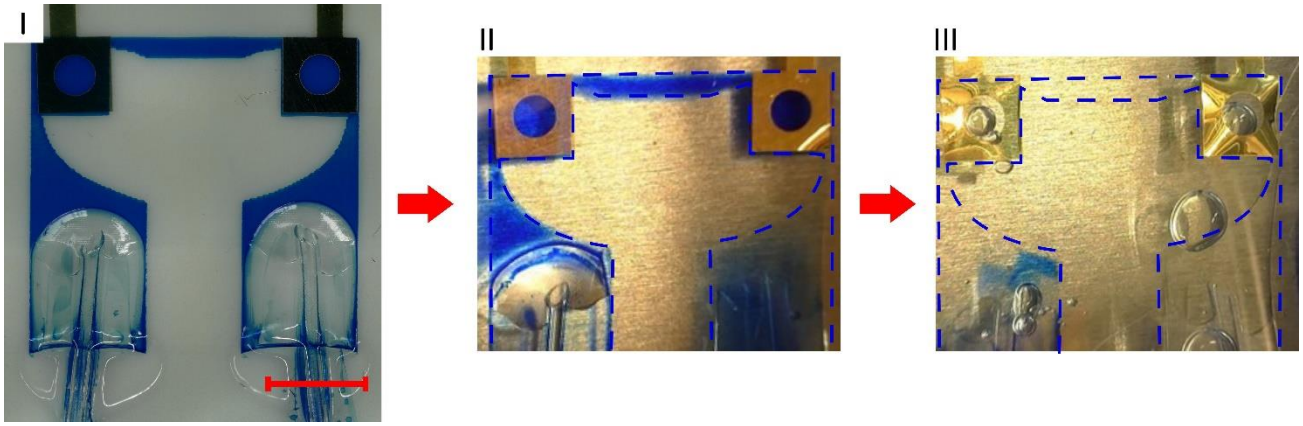

Figure 6. I) Top view of device after fabrication. II) Photo of device during opening process. Right channel is opened, and right actuator pouch is starting to open from the bottom right corner. III) Photo of opened device. Effects of pressurized ethanol are noticeable due to the light reflection on the Mylar foils. Bubbles are caused by infiltration of ethanol between the casted PDMS and the substrate. (scale bar = 5 mm)

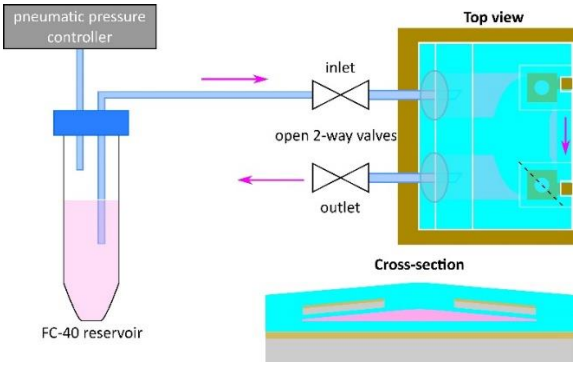

Figure 7. Actuator filling: one device inlet is connected to the dielectric fluid (FC-40) reservoir, along with a valve at each tube. Reservoir pressure is increased to the desired filling pressure (10 mBar) with both valves open, causing the fluid to flow and to push away eventual air bubbles. Once the device is filled, the outlet valve is closed, leading to inner pressure increase. Once pressure is stabilized after few seconds, inlet valve is closed and the actuators are isolated from the reservoir.

Fabrication is completed by filling the opened channels with a dielectric fluid. After drying the ethanol, the same pressure controller is used to fill the channel with a low viscosity, fluorinated dielectric oil (Fluorinert™ Electronic Liquid FC-40 from 3M) as in Figure 7. Two valves are added to the system in order to regulate the filling pressure of the actuators. The outlet valve can be closed in order to impose a static pressure to the channel, and the inlet pressure can isolate the filling volume from the reservoir.

4. FIRST DEVICE ACTUATION

Figure 8 shows setup used to test device actuation. A printed device was filled with FC-40 at 10 mBar initial pressure. Electrical connection to the top electrode is made through the vertical access by bonding a piece of nickel tape to the gold-sputtered Mylar by using a conductive tape (ARcare 90366 from Adhesive Research), and then soldering cables to it. A crocodile clip was then used to connect the bottom electrode underneath the printed device. The electrodes were connected to a high-voltage power supply (Peta-Pico-Voltron[27]). The actuator zipping was captured using a USB camera placed above the device.

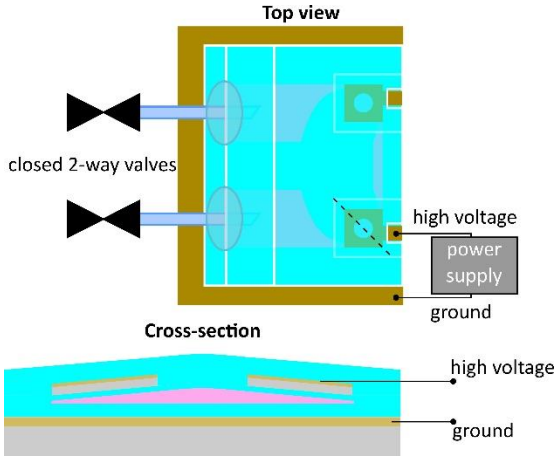

Figure 8. Setup for actuation evaluation

Figure 9 presents two frames from the recorded video. Zipping was achieved in roughly 10 seconds at 2500 V. Once the voltage is reduced to 0 V, the actuator returns to the unactuated state in 20 seconds. The asymmetric time response is caused by the PDMS layers enclosing the fluid adhering to each other during zipping.

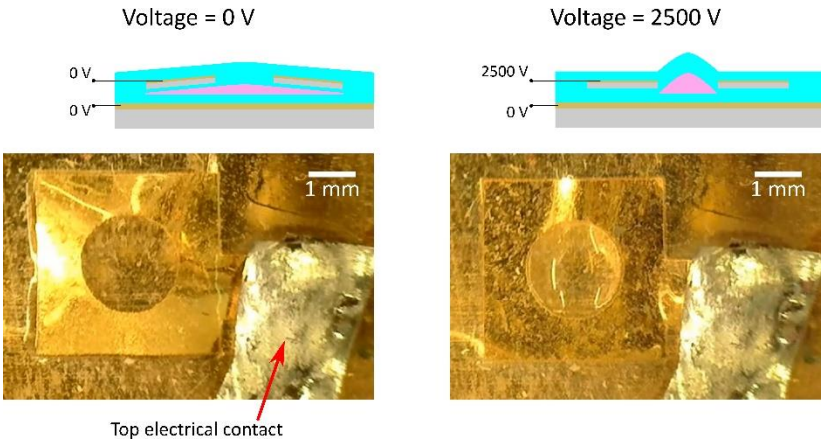

Figure 9. Actuating device. Zipping of top electrode is seen by the change of the light reflection

5. CONCLUSIONS

We presented the first use of inkjet printing for the fabrication of key layers of HAXELs. We printed a sacrificial material in order to obtain fluidic features for actuation and filling, as well as PDMS for stretchable layers. We encapsulated laser-cut Mylar foils with gold deposited on one surface in the fabricated stack, thus providing mechanical support during zipping. We reported the processes followed for channel opening and filling. Finally, we reported the actuation of a fabricated device.

The devices we showed here are a first step towards more complex arrays of HAXELs. Currently pairs of actuators are fluidically linked. This was done to have simple devices to enable testing the opening process. Future development will use a common fluidic system to fill NxN arrays of HAXEL actuators, and the wide tubing inlets will be removed after closing the channels. The integration of Mylar foils with deposited electrodes is also an intermediate solution. It allowed us to evaluate the influence of flexible stiffeners on the fluidic channel opening. Future devices will be made by replacing Mylar with another inkjet-printed flexible dielectric, thus achieving a fully additive fabrication process that will allow complete design flexibility.

ACKNOWLEDGEMENTS

This work was supported by the Swiss National Science Foundation (SNSF), under grant No. 200020_184661. We thank Edouard Leroy for helpful discussions.

REFERENCES

[1] Whitesides, G. M., “Soft Robotics”, Angew. Chem. Int. Ed. 57(16), 4258–4273 (2018).
[2] Yin, J., Hinchet, R., Shea, H. and Majidi, C., “Wearable Soft Technologies for Haptic Sensing and Feedback”, Adv. Funct. Mater., 2007428.
[3] Hines, L., Petersen, K., Lum, G. Z. and Sitti, M., “Soft Actuators for Small-Scale Robotics”, Adv. Mater. 29(13), 1603483 (2017).
[4] Rich, S. I., Wood, R. J. and Majidi, C., “Untethered soft robotics”, Nat. Electron. 1(2), 102–112 (2018).
[5] Pelrine, R. E., Kornbluh, R. D. and Joseph, J. P., “Electrostriction of polymer dielectrics with compliant electrodes as a means of actuation”, Sens. Actuators, A 64(1), 77–85 (1998).
[6] Rosset, S. and Shea, H. R., “Small, fast, and tough: Shrinking down integrated elastomer transducers”, Appl. Phys. Rev. 3(3), 031105 (2016).
[7] Kellaris, N., Venkata, V. G., Smith, G. M., Mitchell, S. K. and Keplinger, C., “Peano-HASEL actuators: Muscle-mimetic, electrohydraulic transducers that linearly contract on activation”, Sci. Robot. 3(14) (2018).

[8] Kellaris, N., Venkata, V. G., Rothemund, P. and Keplinger, C., "An analytical model for the design of Peano-HASEL actuators with drastically improved performance", Extreme Mech. Lett. 29, 100449 (2019).
[9] Taghavi, M., Helps, T. and Rossiter, J., "Electro-ribbon actuators and electro-origami robots", Sci. Robot. 3(25) (2018).
[10] Sato, K. and Shikida, M., "Electrostatic film actuator with a large vertical displacement", Proc. IEEE Micro Electro Mechanical Systems, 1–5 (1992).
[11] Maffli, L., Rosset, S. and Shea, H. R., "Zipping dielectric elastomer actuators: characterization, design and modeling", Smart Mater. Struct. 22(10), 104013 (2013).
[12] Acome, E., Mitchell, S. K., Morrissey, T. G., Emmett, M. B., Benjamin, C., King, M., Radakovitz, M. and Keplinger, C., "Hydraulically amplified self-healing electrostatic actuators with muscle-like performance", Science 359(6371), 61–65 (2018).
[13] Hartmann, F., Penkner, L., Danninger, D., Arnold, N. and Kaltenbrunner, M., "Soft Tunable Lenses Based on Zipping Electroactive Polymer Actuators", Advanced Science, 2003104.
[14] Leroy, E., Hinchet, R. and Shea, H., "Multimode Hydraulically Amplified Electrostatic Actuators for Wearable Haptics", Adv. Mater. 32(36), 2002564 (2020).
[15] Truby, R. L. and Lewis, J. A., "Printing soft matter in three dimensions", Nature 540(7633), 371–378 (2016).
[16] Stano, G. and Percoco, G., "Additive manufacturing aimed to soft robots fabrication: A review", Extreme Mech. Lett., 101079 (2020).
[17] Rossiter, J., Walters, P. and Stoimenov, B., "Printing 3D dielectric elastomer actuators for soft robotics", Proc. EAPAD 7287, (2009).
[18] Manion, C. A., Patel, D. K., Fuge, M. and Bergbrieter, S., "Modeling and Evaluation of Additive Manufactured HASEL Actuators", Proc. IROS, (2018).
[19] O'Neill, M. R., Acome, E., Bakarich, S., Mitchell, S. K., Timko, J., Keplinger, C. and Shepherd, R. F., "Rapid 3D Printing of Electrohydraulic (HASEL) Tentacle Actuators", Adv. Funct. Mater. 30(40), 2005244 (2020).
[20] Baechler, C., Gardin, S., Abuhimd, H. and Kovacs, G., "Inkjet printed multiwall carbon nanotube electrodes for dielectric elastomer actuators", Smart Mater. Struct. 25(5), 055009 (2016).
[21] Chortos, A., Hajiesmaili, E., Morales, J., Clarke, D. R. and Lewis, J. A., "3D Printing of Interdigitated Dielectric Elastomer Actuators", Adv. Funct. Mater. 30(1), 1907375 (2020).
[22] Reitelshöfer, S., Göttler, M., Schmidt, P., Treffer, P., Landgraf, M. and Franke, J., "Aerosol-Jet-Printing silicone layers and electrodes for stacked dielectric elastomer actuators in one processing device", Proc. EAPAD 9798, (2016).
[23] Haghiashtiani, G., Habtour, E., Park, S.-H., Gardea, F. and McAlpine, M. C., "3D printed electrically-driven soft actuators", Extreme Mech. Lett. 21, 1–8 (2018).
[24] Schlatter, S., Grasso, G., Rosset, S. and Shea, H., "Inkjet Printing of Complex Soft Machines with Densely Integrated Electrostatic Actuators", Adv. Intell. Syst. 2(11), 2000136 (2020).
[25] "MYLAR® A datasheet from DuPont Teijin Films.", <https://www.ukinsulations.co.uk/pdfs/Mylar_A_12_-_36mic.pdf> (14 January 2021).
[26] Albuquerque, F. B. and Shea, H., "Influence of humidity, temperature and prestretch on the dielectric breakdown strength of silicone elastomer membranes for DEAs", Smart Mater. Struct. 29(10), 105024 (2020).
[27] Schlatter, S., Illenberger, P. and Rosset, S., "Peta-pico-Voltron: An open-source high voltage power supply", HardwareX 4, e00039 (2018).